RSC Advances

PAPER

View Article Online
View Journal | View Issue

CrossMark click for updates

Cite this: *RSC Adv.*, 2015, **5**, 89083

pH-Sensitive graphene oxide/sodium alginate/polyacrylamide nanocomposite semi-IPN hydrogel with improved mechanical strength

Huijuan Zhang,*[a] Xianjuan Pang[b] and Yuan Qi[a]

It is important and challenging to design a hydrogel that combines mechanical strength and stimuli responsiveness. In this study, graphene oxide (GO) was incorporated into the sodium alginate/polyacrylamide (SA/PAM) hydrogel as the reinforcement to promote the mechanical strength of the hydrogel. The hydrogel was prepared *via in situ* free-radical polymerization in the presence of SA with AM as the monomer and GO as the reinforcement, resulting in a GO/SA/PAM semi-interpenetrating polymer network (IPN). SA, cross-linking agent (*N*,*N*′-methylenebisacrylamide, BIS) and GO proportions were optimized to obtain a hydrogel with superior compressive strength. The $GO_{18}/SA_{0.1}/PAM/BIS_{0.01}$ nanocomposite hydrogel (GO 18 mg, SA 0.1 g, BIS 0.01 g) displayed a compressive strength as high as 65.6 MPa at the compressive deformation of 80%. The hydrogel exhibited pH dependent swelling behavior and a maximum swelling ratio could be observed at pH 4 for the hydrogels with varied GO content. Moreover, the swelling behaviors of the semi-IPN hydrogels are dependent on the GO amounts, and the $GO_{18}/SA_{0.1}/PAM/BIS_{0.01}$ hydrogel sample shows a lower swelling ratio due to its robust inner structures.

Received 23rd September 2015
Accepted 12th October 2015

DOI: 10.1039/c5ra19637j

www.rsc.org/advances

Published on 14 October 2015. Downloaded by Michigan State University on 20/01/2016 00:01:11.

1 Introduction

Responsive hydrogels, known as soft smart or intelligent materials, have been extensively explored as smart soft material for numerous applications.[1–9] The main advantage of these materials is that the reversible non-covalent linker enables hydrogel association and dissociation under external stimuli, which endows the polymeric materials with unique properties such as stimuli-response, injectability and self-healing abilities.[10–12] The reversible and dynamic features of these hydrogels make them suitable and desirable as chemical valves, tissue engineering materials and controlled drug release carrier.[13,14] As one of the stimuli-responsive hydrogels, pH-responsive hydrogels are promising because the pH variation is an important environmental factor in biomedical and other systems.[15–17] Previous studies have shown successful ways in building the responsive hydrogels; however, it is still a challenge to prepare a high-strength hydrogel with responsiveness. Graphene, as a unique 2D nanocarbon material, has aroused great interest due to its extraordinary electronic, thermal and mechanical properties.[18–25]

Graphene oxide (GO), a precursor of graphene-based composites with many oxygenated defects, is a favorable candidate as polymer reinforcement to gain composite materials with improved mechanical performance.[26–29] For example, Yu *et al.* prepared a tough and highly stretchable GO/polyacrylamide (PAM) nanocomposite hydrogel *via in situ* polymerization of AM in an aqueous suspension of GO.[30] As prepared hydrogel exhibited high tensile strength, high toughness and a large elongation at break than that of the chemically cross-linked hydrogels. Nevertheless, the hydrogel cannot respond to the external stimulus, which restricted its application in many potential fields.

Another possible way to obtain high-strength hydrogel is the construction of an interpenetrating polymer network (IPN).[31–33] IPN is conventionally defined as intimate combination of two polymers, which are partially interlaced at the polymer scale but are not covalently bonded to each other. Specifically, a semi-interpenetrating polymer network (semi-IPN or SIPN) is formed if only one of the components is crosslinked. Semi-IPN materials are unique alloys of cross-linked polymers, and the resulting "double network" or semi-IPN systems invariably display excellent mechanical performance that are superior to those of either of the two individual component polymers.[34] Thus, this approach is considered to be a preferable way for designing multi-component hydrogels, which offer the possibility of combining multi-functions of the components and even exhibiting unexpected outstanding properties.[35,36] During the last decade, particular interest has been focused to the semi-IPN containing natural linear macromolecules, *i.e.*, sodium alginate, sodium carboxymethyl

[a]*School of Material and Mechanical Engineering, Beijing Technology Business University, Beijing 100048, China. E-mail: zhanghuijuan@btbu.edu.cn; Tel: +86 10 68985337*

[b]*School of Chemical Engineering and Pharmaceutics, Henan University of Science and Technology, No. 263 Kaiyuan Road, Luoyang 471023, China*

Published on 14 October 2015. Downloaded by Michigan State University on 20/01/2016 00:01:11.

cellulose and carboxymethyl chitosan.[37–47] These natural polysaccharides polyelectrolyte endow the hydrogel with advantageous biocompatibility, biodegradability and non-toxicity.[48,49] Sodium alginate (SA) is an anionic and water soluble natural polymer which is widely used in food, pharmaceuticals and textile printing.[50] SA can also be used as a hydrophilic polymer and a pH-responsive component for obtaining pH-sensitive hydrogels.[51]

Therefore, it is important to design and construct a biocompatible, pH-sensitive semi-IPN composite hydrogel with superior mechanical performance. To this end, a pH-responsive GO/PAM/SA composite hydrogel with interpenetrating polymer network was designed and synthesized. For the fabrication of the hydrogel, AM was polymerized in the presence of GO and SA, which formed a hydrogel by a chemical cross-linker (BIS). In the network, SA acted as one of the constituent and pH-sensitive moiety simultaneously. GO was included as the reinforcement, aiming to achieve desirable mechanical strength. The compressive tests of the composite hydrogel were investigated in terms of the contents of SA, BIS and GO. The pH-sensitive swelling behaviors of the hydrogels were studied. The rheology, morphologies, and the possible interactions between the components were also investigated. On the basis of the characterizations, a possible mechanism for the formation and pH responsiveness was proposed.

2 Experimental

2.1 Materials

Graphene oxide (diameter: 0.5–5 μm; thickness: 0.8–1.2 nm) was purchased from Nanjing XFNANO Materials Tech Co., Ltd. Sodium alginate (SA) (200 mPa s CP), acrylamide (AM), ammonium persulfate (APS), *N*,*N*′-methylenebisacrylamide (BIS), citric acid and sodium phosphate dibasic (Na_2HPO_4) were purchased from Sinopharm Chemical Reagent Co. Ltd (SCRC) and used without further purification.

2.2 Preparation of the composite hydrogels

Hydrogels were prepared by a simple mixture and solution polymerization using initial solutions consisting of monomers (GO, AM and SA), crosslinker (BIS) and initiator (APS). Typical procedure was as follows: firstly, the desired amount of dried GO was exfoliated and dispersed in 15 mL of water by sonication for 2 h using a SK2510HP ultrasonicator. Successively, 0.10 g SA was added and dissolved in the above GO aqueous dispersion under magnetic stirring and sonication at room temperature until the solution became uniform. Then 3.6 g AM, 0.010 g APS and 0.010 g BIS were added and stirred at 0 °C. After magnetic stirring for 2 h under 0 °C, the homogeneous mixture solutions were transferred into a glass tube and kept for hydrogel formation at 80 °C for 2 h. After the completion of the hydrogel preparation, the hydrogels in their cylinder form, were taken out of the glass tube and put into a beaker, which contained large amount of de-ionized (DI) water. To remove the unreacted monomers, the water was renewed every 6 hours for 2 weeks. After the hydrogel formation, the composite hydrogels, in their cylindrical form, were taken out of the glass tube and put into DI water to remove homopolymers and unreacted monomers (Table 1). In this paper, hydrogels are expressed as $GO_a/SA_b/PAM/BIS_c$ hydrogels, where *a*, *b*, *c* represents the feed amount of GO, SA and BIS, respectively.

Table 1 The feed compositions of the hydrogels

Sample	AM (g)	SA (g)	APS (g)	BIS (g)	GO (g)	H_2O (mL)
$SA_{0.1}/PAM/BIS_{0.01}$	3.6	0.10	0.010	0.010	—	15
$SA_{0.1}/PAM/BIS_{0.02}$	3.6	0.10	0.010	0.020	—	15
$SA_{0.1}/PAM/BIS_{0.03}$	3.6	0.10	0.010	0.030	—	15
$SA_{0.2}/PAM/BIS_{0.01}$	3.6	0.20	0.010	0.010	—	15
$SA_{0.3}/PAM/BIS_{0.01}$	3.6	0.30	0.010	0.010	—	15
$GO_{12}/SA_{0.1}/PAM/BIS_{0.01}$	3.6	0.10	0.010	0.010	0.012	15
$GO_{18}/SA_{0.1}/PAM/BIS_{0.01}$	3.6	0.10	0.010	0.010	0.018	15
$GO_{24}/SA_{0.1}/PAM/BIS_{0.01}$	3.6	0.10	0.010	0.010	0.024	15

2.3 Characterization

The samples for FT-IR and SEM analysis were all pretreated by freeze-drying technique. For FT-IR characterization, the samples were mixed with KBr powder. Then the mixture was ground in agate mortar evenly and a typical platelet for FT-IR was obtained in the mold. Data were collected over 32 scans at 8 cm^{-1} resolution. The morphology of specimens was observed on a QUANTA FEG 250 scanning electron microscope (SEM). Before observation, the freeze-dried samples were cut by a microtome. Then the sliced samples were fixed into sample table for sputter coating with gold under vacuum. The images were obtained under an accelerating power of 10 kV. Thermogravimetric (TG) analyses were conducted with Q5000IR, heating samples from ambient temperature to 700 °C at the heating rate of 20 °C min^{-1} in a nitrogen atmosphere. Rheological properties of the hydrogels were conducted with HAAKE MARS III rheometer using parallel plates of diameter 20 mm at 20 °C. The gap between the two parallel plates was set at 1 mm. The dynamic strain sweep from 0.1% to 200% was carried out at an angular frequency of 1 Hz. The frequency sweep was performed over the frequency range of 0.01–10 Hz.

2.4 Measurement of swelling ratio and water retention

Before the swelling experiment, the hydrogels were cut into small pieces and dried by lyophilization: firstly, the hydrogels were set in the chamber at −56 °C for 12 hours for pre-freezing. Afterwards, the frozen hydrogels were vacuum dried for 48 hours to a constant weight. The swelling ratios of hydrogel samples were measured in buffer solutions at various pH values using a gravimetric method. Here, all the initial dry hydrogels were tested with the same weight (100 mg) and the same water volume (1000 mL). The buffer solutions with pH from 2.2 to 8 were prepared by changing the molar ratio of citric acid to sodium phosphate dibasic. The dried hydrogels were immersed in water until their weight became constant. The hydrogels were then removed from the water and their surfaces were blotted

 This journal is © The Royal Society of Chemistry 2015

Published on 14 October 2015. Downloaded by Michigan State University on 20/01/2016 00:01:11.

with filter paper before weighed. The swelling ratio was calculated with the following equation:

$$\text{Swelling ratio} = \frac{W_s - W_d}{W_d} \quad (1)$$

where W_d and W_s represent the weights of the dried hydrogel and the hydrogel at swelling equilibrium state, respectively. All the experiments were carried out in triplicate, and the average values were reported.

Typical procedure for deswelling experiment was conducted as follows: 100 mg hydrogel sample was immersed in an aqueous solution at room temperature for 24 hours to reach swelling equilibrium. The swollen gels were blotted with filter paper for further deswelling experiment. The deswelling behavior of the hydrogel was studied by recording the weight of water in the hydrogels at determined time. Water retention was calculated as:

$$\text{Water retention} = \frac{W_t - W_d}{W_s - W_d} \quad (2)$$

where W_t is the weight of the hydrogel at a given time interval during the course of deswelling after the swollen hydrogel had been quickly transferred into neutral water. In all cases three parallel samples were used and the averages are reported in this paper.

2.5 Compressive tests of hydrogels

The mechanical properties of the hydrogels were tested using a CMT6104 universal testing machine. For the compressive tests, the hydrogel samples (column, with a diameter of 12 mm and height of 10 mm) were placed between the self-leveling plates. The samples were compressed at a rate of 20 mm min^{-1} until the compression ratio reached 80%.

3 Results and discussion

GO/SA/PAM nanocomposite hydrogels were prepared *via* free radical polymerization with AM as the monomer and GO as reinforcement in the presence of SA, which acted as the first network of the semi-IPN. The advantages of incorporating SA into the nanocomposite hydrogel were considered to be due to the following properties: (1) as a typical anionic linear natural polymer, SA is pH sensitive and biodegradable, which endows the nanocomposite hydrogels with the stimuli responsiveness and biocompatibility and thus broadens their applications. (2) The inclusion of SA into the hydrogel is supposed to promote the mechanical properties of the hydrogel.

The semi-IPN SA/PAM hydrogels in the absence of GO, with varied proportions of SA and cross-linking agent (BIS), were firstly prepared to optimize the preparation conditions. The compressive strength of as-prepared hydrogels was measured to describe the differences between the samples. The obtained hydrogels for compressive tests were tested in equilibrium swelling state. The analysis of variance (ANOVA) was used to evaluate the contributions of SA and BIS concentrations to the compressive strength. The ANOVA statistic results showed the effects of SA and BIS concentrations were significant, since these effects presented p-values smaller than 0.01. This means that the probability of the null hypothesis to be true is less than 1%. As shown in Fig. 1(a), the compressive strength of the hydrogels goes down with the increasing SA amounts. The similar result was also reported by Gong *et al.*,[35] who found that the molar ratio of the first to the second network is crucial for obtaining the DN mechanically strong gels. However, they did not provide possible explanations. It is known that the effective stress dissipation is the key to the toughness of a material.[35] The above results showed that the mechanical stress was effectively dissipated in the hydrogel with the lower SA content. It could also be observed that the hydrogels with lower BIS concentration exhibited higher compressive strength (Fig. 1(b)). Generally speaking, the higher BIS content would result in an increase of crosslinking density, which would restrict the motion of macromolecular chains. Unsurprisingly, the hydrogel with higher content of crosslinking agent, *i.e.*, $SA_{0.1}$/PAM/$BIS_{0.03}$, failed to undergo a large deformation due to the low mobility of its cross-linking polymer chains in the network.

As shown in the previous section, the semi-IPN $SA_{0.1}$/PAM/$BIS_{0.01}$ hydrogel sample (SA 0.1 g and BIS 0.01 g) showed advantageous mechanical properties. Therefore, the recipe was selected to investigate the effects of GO contents on the compressive strength, as shown in Fig. 2. The effect of GO proportions on the compressive strength is also analyzed by ANOVA. The results confirmed that the observed changes on the compressive strength could be ascribed to changes in the level

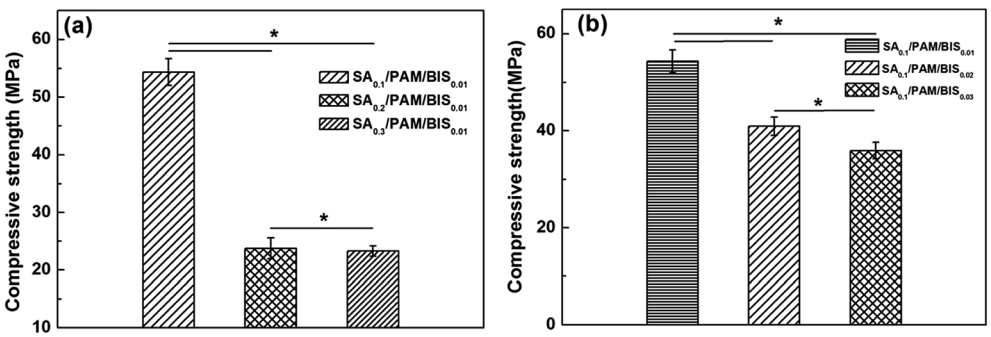

Fig. 1 Compressive strength of SA/PAM/BIS hydrogels with varied amounts of (a) SA and (b) BIS. * Indicates statistically significant difference between the varied SA or BIS concentrations with $p < 0.01$. Results are presented as mean ± s.d. ($n = 3$).

Published on 14 October 2015. Downloaded by Michigan State University on 20/01/2016 00:01:11.

of GO concentrations. As indicated in Fig. 2, the compressive strength firstly increased and then declined to a certain extent. The dependence of GO content on the compressive properties of $GO/SA_{0.1}/PAM/BIS_{0.01}$ was probably related to the dispersion of GO and its interfacial interaction with polymer chains, which will be discussed below.

To visualize the differences between the compressive strength of $SA_{0.1}/PAM/BIS_{0.01}$ and $GO_{18}/SA_{0.1}/PAM/BIS_{0.01}$ hydrogels, the photographs of both samples under pressure were taken and shown in Fig. 3. $GO_{18}/SA_{0.1}/PAM/BIS_{0.01}$ hydrogel displays excellent performance in ductility, which is tough enough to withstand high deformations in compression without obvious damage. As shown in Fig. 3(a)–(c), $GO_{18}/SA_{0.1}/PAM/BIS_{0.01}$ hydrogel was not destroyed by compressing, even with an extremely high strain. Upon removing pressure, $GO_{18}/SA_{0.1}/PAM/BIS_{0.01}$ hydrogel quickly recovered its original shape. In contrast, $SA_{0.1}/PAM/BIS_{0.01}$ hydrogel, prepared in the absence of GO, was crushed by compressing because of its brittleness (Fig. 3(d)–(f)).

TG analysis is performed to indicate the changes of thermal stability of SA, GO sheets, $SA_{0.1}/PAM/BIS_{0.01}$ and $GO/SA_{0.1}/PAM/BIS_{0.01}$ hydrogels (Fig. 4). The mass loss peak for GO at about 200 °C can be ascribed to the pyrolysis of the labile oxygen containing functional group.[52,53] Additionally, GO content in $GO/SA_{0.1}/PAM/BIS_{0.01}$ IPN gel can also be estimated to be 1.8 wt% according to TGA measurements. This value is a little higher than the original feed ratio (0.48 wt% GO). It reveals that GO sheets all participated in the cross-linking reaction indicating rather high reaction efficiency in water.[28] It is observable that the thermal stability was raised for the composite hydrogel with GO as enhancement, suggesting strong interactions between GO sheets and polymer chains.

FT-IR could provide important information about the successful cross-linking reaction and the possible interactions between GO and polymer chains. For comparison, the FT-IR spectra of GO, $SA_{0.1}/PAM/BIS_{0.01}$ and $GO/SA_{0.1}/PAM/BIS_{0.01}$ hydrogel samples with the gradient GO concentrations were shown in Fig. 5. The obvious peaks at 1732, 1401, 1226 and 1046 cm^{-1} in the FT-IR spectrum of GO powder were attributed to C=O carbonyl stretching, aromatic C=C stretching, O–H deformation vibration, and asymmetric and symmetric C–O stretching in C–O–C group, respectively. In the FT-IR spectrum of $SA_{0.1}/PAM/BIS_{0.01}$, the bands at 3390, 2923, 2855 cm^{-1} in the high-frequency region were characteristic of N–H stretching and

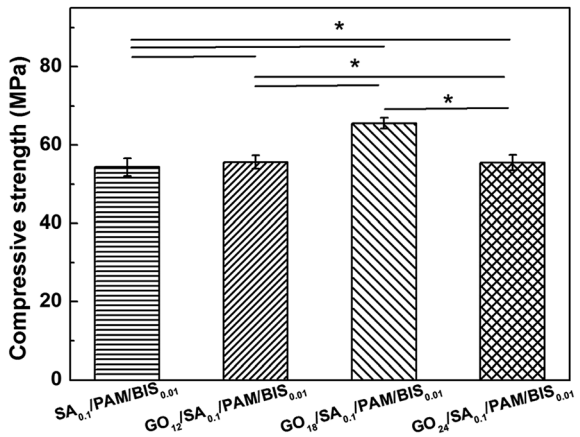

Fig. 2 Compressive strength of $GO/SA_{0.1}/PAM/BIS_{0.01}$ hydrogels with varied amounts of GO. * Indicates statistically significant difference between the varied GO concentrations with $p < 0.01$. Results are presented as mean ± s.d. ($n = 3$).

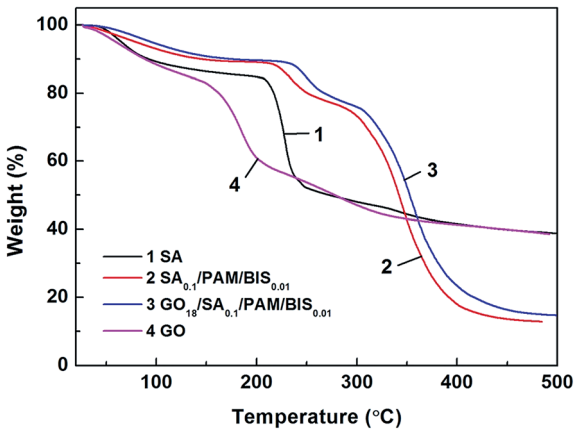

Fig. 4 TGA curves of SA, GO sheets, $SA_{0.1}/PAM/BIS_{0.01}$ and $GO/SA_{0.1}/PAM/BIS_{0.01}$ hydrogels.

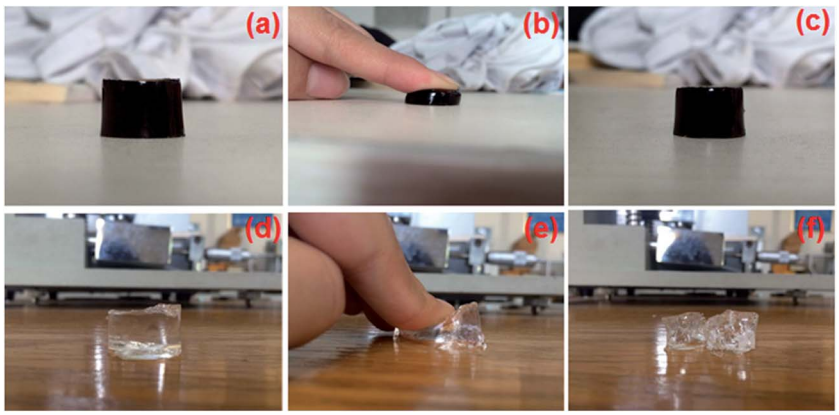

Fig. 3 Photographs of $GO_{18}/SA_{0.1}/PAM/BIS_{0.01}$ (a–c) and $SA_{0.1}/PAM/BIS_{0.01}$ hydrogels (d–f) under pressure.

 This journal is © The Royal Society of Chemistry 2015

Published on 14 October 2015. Downloaded by Michigan State University on 20/01/2016 00:01:11.

asymmetric and symmetric vibration of C–H stretching, respectively. The strong peak at 890 cm^{-1}, which appears only in the spectrum of AM monomer due to the existence of $=CH_2$,[54] does not appear in the spectrum of all the tested hydrogels, confirming that AM monomer has been polymerized. Moreover, the characteristic absorption bands at 1059 and 1095 cm^{-1} could be ascribed to the stretching vibration C–O–C ether groups in SA, respectively. These data were in good accordance with the literature[55] and indicated the successful incorporation of SA into the hydrogel network. The peak at 1612 cm^{-1} can be ascribed to NH_2 bending vibration in PAM.[30] It is worth noting that the peaks at 1612 cm^{-1} shifted and broadened with the increasing content of GO sheets. The shift could be ascribed to the presence of the hydrogen bonding interactions between the N–H bond of $SA_{0.1}$/PAM/$BIS_{0.01}$ and O–H bond of GO nanosheets.[56,57]

SEM is very helpful in characterizing the inner morphologies of the hydrogels. To prepare samples for SEM observation, it is necessary to treat the hydrogels by freeze-drying to make sure the porous structure is well preserved. Moreover, the freeze-dried samples are sliced by a microtome, which guarantee the bulk, instead of the surface of the hydrogel was observed. The hydrogel samples with varied crosslinking agent contents displayed distinct morphologies as shown in Fig. 6(a)–(c). After removing water, SEM images of $SA_{0.1}$/PAM/$BIS_{0.01}$ hydrogel show characteristic porous structure with the diameter ranging from 100 to 150 μm (Fig. 6(a)). The inner structure exhibits a thick block with sparse pores dispersed. Interestingly, the pore size of the $SA_{0.1}$/PAM/$BIS_{0.02}$ hydrogel becomes smaller, implying a tighter structure of the hydrogel (Fig. 6(b)). As the crosslinking agent concentration was further increased, the inner structure of the hydrogel transformed into a net-like morphology, implying a denser structure (Fig. 6(c)). The morphology evolution of the hydrogels suggested that the inner structure was closely dependent on the BIS proportion. It seemed that the inner structure of the $SA_{0.1}$/PAM/$BIS_{0.03}$ was finer and interconnected to each other to a greater extent, which implied that the polymer chains were greatly restricted. This trend was in good agreement with the compressive strength dependence on the BIS content. Comparing Fig. 6(a) and (d), it could be found that GO_{18}/$SA_{0.1}$/PAM/$BIS_{0.01}$ presented a robust three dimensional structure. The pore diameter was evenly distributed, which ensured the stress transfer and was favorable for enhancing the mechanical properties. It should be noted that no obvious aggregation of GO nanosheets is observed, indicating a uniform distribution of GO sheets in the hydrogel.

Fig. 6(e) shows the possible concise mechanism for the formation of GO/$SA_{0.1}$/PAM/$BIS_{0.01}$ nanocomposite semi-IPN hydrogel. For the $SA_{0.1}$/PAM/$BIS_{0.01}$ hydrogel, covalently crosslinked PAM was formed in the presence of SA. Two types of polymer are partially intertwined at the polymer scale. As confirmed previously by FT-IR results, hydrogen bonding interaction existed in the GO/SA/PAM hydrogels. Upon the involvement of GO sheets, the emerging crosslinking points were formed due to the GO participating in the polymerization.[30,58] Additionally, the functional groups on the surface the

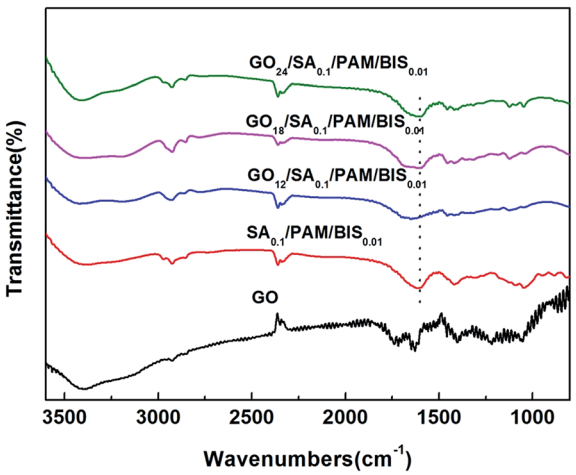

Fig. 5 FT-IR spectra of GO sheets, $SA_{0.1}$/PAM/$BIS_{0.01}$ and GO/$SA_{0.1}$/PAM/$BIS_{0.01}$ hydrogels.

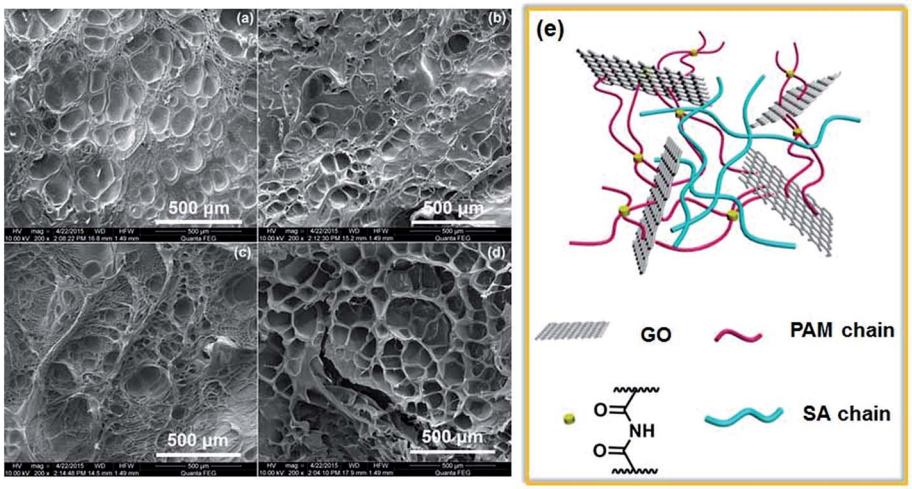

Fig. 6 SEM images of the hydrogels. (a) $SA_{0.1}$/PAM/$BIS_{0.01}$, (b) $SA_{0.1}$/PAM/$BIS_{0.02}$, (c) $SA_{0.1}$/PAM/$BIS_{0.03}$ and (d) GO_{18}/$SA_{0.1}$/PAM/$BIS_{0.01}$ hydrogel, (e) schematic of GO/$SA_{0.1}$/PAM/$BIS_{0.01}$ composite semi-IPN hydrogels.

Published on 14 October 2015. Downloaded by Michigan State University on 20/01/2016 00:01:11.

GO nanosheets offer hydrogen bonding interactions with the side chains of the polymer chains. These two factors contributed collaboratively to the enhanced mechanical properties of the nanocomposite hydrogel.

Rheology was utilized to characterize the viscoelastic behaviors of the hydrogels with the varied GO contents. To this end, the dependence of storage moduli (G') on time, strain and angular frequency was measured, where G' could reflect the elastic properties of the sample. It was confirmed that the shear modulus of the $SA_{0.1}/PAM/BIS_{0.01}$ initially increased after the introduction of GO sheets, and then experienced a decline when the content was further growing (Fig. 7(a)). This is consistent with the previous compressive tests of the hydrogels. Moreover, towards 1% of strain, obvious changes of the storage moduli were not witnessed with the prolonging time, indicating a minimal stress relaxation of the hydrogels (Fig. 7(b)). The frequency sweeping results also demonstrated the reinforcing effect of GO nanosheets (Fig. 7(c)). Moreover, the characteristic viscoelastic behaviors of the gels was confirmed, *i.e.* the values of G' varied little with angular frequency, and G' was significantly larger than G'' over all measured frequencies.

SA is a natural polyelectrolyte with many carboxylic groups in its molecular chain, which exhibit reversible hydration/dehydration in basic/acidic medium. Therefore, we investigated the influence of the pH values of the medium on the swelling ratios for the GO/SA/PAM hydrogels in the pH range of 2.2–8. It could be observed from Fig. 8 that the swelling ratio of the semi-IPN $SA_{0.1}/PAM/BIS_{0.01}$ hydrogel samples increased in the lower pH values, *i.e.*, from 2 to 4. This raise in the swelling ratio may be ascribed to the change in the dissociation degree of carboxylic groups and the formation of the hydrogen bonds between –COOH and –CONH– groups: at lower pH values (below the pK_a of carboxylic groups, ~4.6), the $–COO^-$ groups in SA are protonated to –COOH groups. Meanwhile, the hydrogen bonds between –COOH and –CONH– groups are formed. Remarkably, these factors played crucial roles in the diminishing polymer/water interactions as well as the swelling ratio. The lower pH values of the medium, the stronger the hydrogen bonds and thus the smaller the swelling ratio of the hydrogels. When pH value is increased to ~4, the carboxylic acid groups become ionized and the electrostatic repulsion between the molecular chains is predominate, which leads to the network expanding more, where a maximum swelling ratio is observed for the SA/PAM hydrogels. Beyond this value, a screening effect of the counter ions, *i.e.*, $GO_{12}/SA_{0.1}/PAM/BIS_{0.01}$ at pH 5–6, Na^+, shields the charge of the carboxylate anions, which may prevent an efficient repulsion.[37] As a result, a remarkable decrease in equilibrium swelling is observed. The similar phenomenon was also reported by Ma *et al.*[37]

The similar tendency is also observed for the GO incorporated nanocomposite hydrogels. However, the GO/SA/PAM hydrogel showed less sensitive response toward pH variations. This may be associated with the complex interactions of the network due to the inclusion of GO sheets. It was reported that the oxygen-containing groups on GO surface would participated in the radical chain transfer reactions during the free-radical polymerization, which resulted in the grafting of PAM macromolecules onto the layered GO sheets.[37,58] In other words, these GO sheets acted as fresh chemical crosslinking points in the hydrogel formation and intercalated into the polymer networks

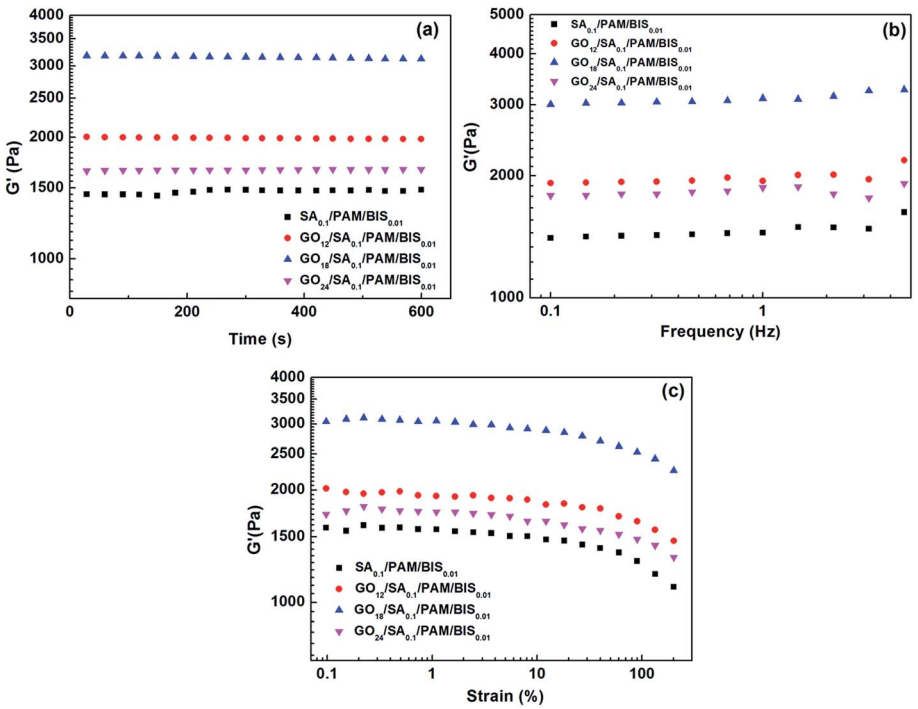

Fig. 7 Dependence of storage modulus (G') on (a) time, (b) strain and (c) angular frequency for $SA_{0.1}/PAM/BIS_{0.01}$ hydrogel and $GO/SA_{0.1}/PAM/BIS_{0.01}$ hydrogels.

 This journal is © The Royal Society of Chemistry 2015

Published on 14 October 2015. Downloaded by Michigan State University on 20/01/2016 00:01:11.

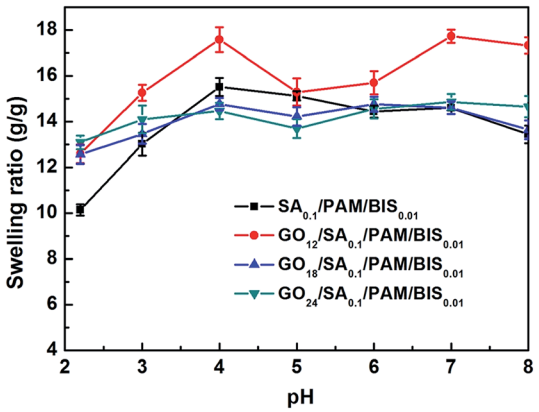

Fig. 8 Swelling ratio of hydrogels as a function of pH values of the medium.

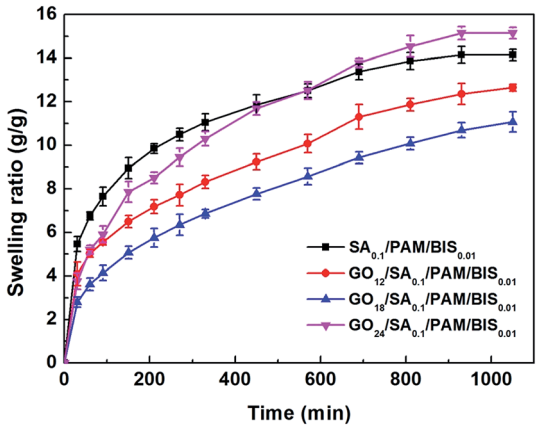

Fig. 9 Swelling behaviors of $SA_{0.1}/PAM/BIS_{0.01}$ and $GO/SA_{0.1}/PAM/BIS_{0.01}$ hydrogels in distilled water.

of the hydrogel. Additionally, SA chains were entrapped and entangled to a great extent, which promoted the polymer–polymer interactions and hindered the SA interaction with water.

To evaluate the swelling behaviors of the hydrogels, the hydrogels were swelled in water and the weight was measured at determined time to trace the swelling ratio with the prolonging time (Fig. 9). As expected, the swelling process of all the tested hydrogel samples consists of two regimes: the first one is a relatively quickly increasing process and the subsequent one is a slow-increasing process. The swelling equilibrium of the hydrogel samples could be achieved within about 1000 min. Moreover, it could be observed from Fig. 9 that the swelling ratio of the composite hydrogels presented a nonmonotonic variation with the increasing GO proportion, that is, the swelling ratio firstly declined with the increasing GO loadings, and then increased with the GO content of 24 mg. It is accepted that the swelling behavior of the hydrogel depended significantly on the crosslinked density of the gel network.[59,60] Generally, the hydrogel with higher cross-linking density, where the free motion of the polymer chains is restricted to a great extent, shows a lower swelling capacity due to the weakened polymer/water affinity. In $GO/SA_{0.1}/PAM/BIS_{0.01}$ hydrogel, GO nanosheets could act as a kind of cross-linker and formed plenty of cross-link points, which gave rise to a reduction of the swelling ratio. The differences in swelling behaviors confirmed the more robust network of the $GO/SA_{0.1}/PAM/BIS_{0.01}$ hydrogel.

The reasons of the nonmonotonic variation of the swelling ratio with the GO loadings might be ascribed to the following factors. There are two competing effects in the GO/SA/PAM nanocomposite hydrogels in terms of swelling capacity. On the one hand, the incorporation of the GO sheets tends to interact with PAM chains and increases the cross-linked density, which would result in the decreased swelling ratio.[61] On the other hand, the GO sheets containing plenty of functional groups, *i.e.* carboxylic, carboxyl, hydroxyl and ether groups on the surface, which could dramatically increase the density of the hydrophilic groups of the polymer networks.[62] When the GO loadings were low, the cross-linked density increased significantly with the increase of the GO loadings, which resulted in the denser inner structures of the GO/SA/PAM network and thus the decreased swelling ratio. As the GO loadings were further increased, *i.e.* 24 mg, the positive effect of the GO nanosheets on the swelling capacity became apparent. The swelling ratio of the $GO_{24}/SA_{0.1}/PAM/BIS_{0.01}$ hydrogel increased and was even higher than that of the conventional SA/PAM hydrogel.

The swelling capacities of $SA_{0.1}/PAM/BIS_{0.01}$ and $GO/SA_{0.1}/PAM/BIS_{0.01}$ hydrogels with various GO loadings in deionized water and in 0.9 wt% NaCl solution are shown in Fig. 10. ANOVA statistic results revealed a significant effect of gel type and medium with $p < 0.01$, respectively. The hydrogel samples showed satisfactory salt tolerance, that is, all the samples exhibited higher swelling ratio in 0.9 wt% NaCl solution than that in deionized water. It was reported by Huang *et al.*[26] that the swelling ratio of the graphene oxide/poly(acrylic acid-*co*-acrylamide) hydrogels in 0.9 wt% NaCl solution declined sharply compared to that in deionized water. In this hydrogel system, SA was incorporated as a polyelectrolyte in small amount, *i.e.*, 2.7

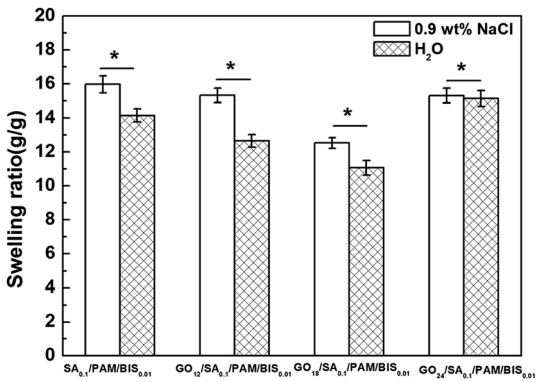

Fig. 10 Swelling capacities of $SA_{0.1}/PAM/BIS_{0.01}$ and $GO/SA_{0.1}/PAM/BIS_{0.01}$ hydrogels with various GO loadings in deionized water and in 0.9 wt% NaCl solution. * Indicates statistically significant difference between water and 0.9 wt% NaCl solution with $p < 0.01$. Results are presented as mean ± s.d. ($n = 3$).

Published on 14 October 2015. Downloaded by Michigan State University on 20/01/2016 00:01:11.

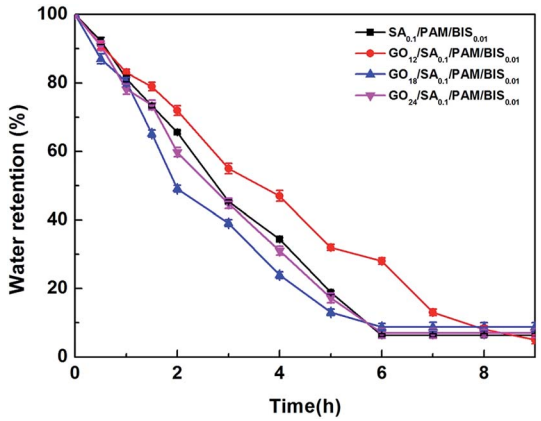

Fig. 11 Deswelling behaviors of $SA_{0.1}$/PAM/$BIS_{0.01}$ and GO/$SA_{0.1}$/PAM/$BIS_{0.01}$ hydrogels.

wt% of SA to the total amount of SA and AM in $SA_{0.1}$/PAM/$BIS_{0.01}$ sample. The majority constituent of the hydrogel was PAM, which is neutral and showed little sensitiveness towards ionic strength. The dried gel absorbs large amount of water due to its affinity with water molecules. The gel deswells with the prolonging time if exposed to the air, which is caused by the evaporation of the water molecules. The deswelling rate is an important factor and, in particular, high rates are needed in many applications. The deswelling behavior of the hydrogels was evaluated by measuring the swelling ratios of the hydrogels at determined time. The deswelling curves of the hydrogels are shown in Fig. 11. It could be observed that the investigated hydrogel samples, unfilled and GO filled, displayed a fast deswelling rate and all the samples kept stable within 8 hours. Considering the favorable salt resistance and fast deswelling rate, the semi-IPN nanocomposite hydrogels may be potentially applied in hygienics and agricultural areas.

4 Conclusions

In summary, a pH-responsive and mechanically strong semi-IPN hydrogel, with SA as the pH sensitive moiety and GO sheets as the reinforcement, was successfully fabricated. The semi-IPN hydrogel was prepared by controlling the amount of SA, crosslinker and GO nanosheets. The cross-linking reaction is highly effective, resulting in a hydrogel network with a porous structure. Notably, the nanocomposite semi-IPN hydrogels displayed promoted compressive strength owing to the hydrogen bonding between GO sheets and polymer chains. This interaction was also confirmed by the FT-IR results, which indicated peak shifts of amino groups in GO doped nanocomposite hydrogels. The excessive amount of GO, however, would exert an unfavorable effect on the mechanical properties. The specific SA component endowed the hydrogels with pH sensitive swelling ratio, which was dependent greatly on the GO content. Considering the pH-sensitivity and the superior mechanical properties of the semi-IPN hydrogels, it is expected that the present hydrogel could offer new insights into the smart soft matter fields. The preparation method may also be extended to other hydrogels, and thus enlarge the application of the nanocomposite hydrogel materials sensors and actuators.

Acknowledgements

We acknowledge financial support from National Nature Science Foundation of China (no. 21104040).

References

1 D. J. Pochan, J. P. Schneider, J. Kretsinger, B. Ozbas, K. Rajagopal and L. Haines, *J. Am. Chem. Soc.*, 2003, **125**, 11802–11803.
2 G. Chen and A. S. Hoffman, *Nature*, 1995, **273**, 49–52.
3 S. Keun, K. Sung, W. Young, H. Jin, Y. Ji and H. Soon, *Biomaterials*, 2004, **25**, 2393–2398.
4 A. Gutowska, Y. H. Bae, H. Jacobs, J. Feijen and S. W. Kim, *Macromolecules*, 1994, **27**, 4167–4175.
5 F. llmain, T. Tanaka and E. Kokufuta, *Nature*, 1991, **349**, 400–401.
6 C. Tsitsilianis, *Soft Matter*, 2010, **6**, 2372–2388.
7 X. L. He, S. Yu, Y. Y. Dong, F. Y. Yan and L. Chen, *J. Mater. Sci.*, 2009, **44**, 4078–4086.
8 G. T. Gotzamanis, C. Tsitsilianis, S. C. Hadijyannakou, C. S. Patrickios and R. Lubetsky, *Macromolecules*, 2006, **39**, 678–683.
9 Z. S. Ge, J. M. Hu, F. H. Huang and S. Y. Liu, *Angew. Chem., Int. Ed.*, 2009, **48**, 1798–1802.
10 Z. K. Wang, L. H. Wang, J. T. Sun, L. F. Han and C. Y. Hong, *Polym. Chem.*, 2013, **4**, 1694–1699.
11 S. Kiyonaka, K. Sada, I. Yoshimura, S. Shinkai, N. Kato and I. Hamachi, *Nat. Mater.*, 2004, **3**, 58–64.
12 K. Y. Lee and S. H. Yuk, *Prog. Polym. Sci.*, 2007, **32**, 669–754.
13 Z. X. Zhang, K. L. Liu and J. Li, *Angew. Chem., Int. Ed.*, 2013, **52**, 6180–6184.
14 J. Li and X. J. Loh, *Adv. Drug Delivery Rev.*, 2008, **60**, 1000–1017.
15 Z. Q. Li, J. F. Shen, H. W. Ma, X. Lu, M. Shi, N. Li and M. X. Ye, *Soft Matter*, 2012, **8**, 3139–3145.
16 H. Bai, C. Li, X. L. Wang and G. Q. Shi, *Chem. Commun.*, 2010, **46**, 2376–2378.
17 H. C. Chiu, Y. F. Lin and S. H. Hung, *Macromolecules*, 2002, **35**, 5235–5242.
18 J. H. Chen, C. Jang, S. D. Xiao, M. Ishigami and M. S. Fuhrer, *Nat. Nanotechnol.*, 2008, **3**, 206–209.
19 A. A. Balandin, S. Ghosh, W. Z. Bao, I. Calizo, D. Teweldebrhan, F. Miao and C. N. Lau, *Nano Lett.*, 2008, **8**, 902–907.
20 R. R. Nair, P. Blake, A. N. Grigorenko, K. S. Novoselov, T. J. Booth, T. Stauber, N. M. R. Peres and A. K. Geim, *Science*, 2008, **320**, 1308.
21 C. Lee, X. D. Wei, J. W. Kysar and J. Hone, *Science*, 2008, **321**, 385–388.
22 S. V. Dubonos, I. V. Grigorieva and A. A. Firsov, *Science*, 2004, **306**, 666–669.
23 A. K. Geim, *Science*, 2009, **324**, 1530–1534.

 This journal is © The Royal Society of Chemistry 2015

Published on 14 October 2015. Downloaded by Michigan State University on 20/01/2016 00:01:11.

24 C. N. R. Rao, A. K. Sood, K. S. Subrahmanyam and A. Govindaraj, *Angew. Chem., Int. Ed.*, 2009, **48**, 7752–7777.
25 M. J. Allen, V. C. Tung and R. B. Kaner, *Chem. Rev.*, 2010, **110**, 132–145.
26 Y. W. Huang, M. Zeng, J. Ren, J. Wang, L. R. Fan and Q. Y. Xu, *Colloids Surf., A*, 2012, **401**, 97–106.
27 J. Shen, B. Yan, T. Li, Y. Long, N. Li and M. Ye, *Composites, Part A*, 2012, **43**, 1476–1481.
28 S. Sun and P. Wu, *J. Mater. Chem.*, 2011, **21**, 4095–4097.
29 L. Zhang, Z. Wang, C. Xu, Y. Li, J. Gao, W. Wang and Y. Liu, *J. Mater. Chem.*, 2011, **21**, 10399–10406.
30 R. Q. Liu, S. M. Liang, X. Z. Tang, D. Yan, X. F. Li and Z. Z. Yu, *J. Mater. Chem.*, 2012, **22**, 14160–14167.
31 M. A. Ayman, E. M. Nermine and K. F. Arndt, *J. Polym. Res.*, 2006, **13**, 53–63.
32 A. G. Leontine and M. Martin, *Polym. Bull.*, 1992, **27**, 681–688.
33 A. A. Artyukhov, M. I. Shtilman, A. N. Kuskov, A. P. Fomina, D. E. Lisovyy, A. S. Golunova and A. M. Tsatsakis, *J. Polym. Res.*, 2011, **18**, 667–673.
34 D. Myung, D. Waters, M. Wiseman, P. E. Duhamel, J. Noolandi, C. N. Ta and C. W. Frank, *Polym. Adv. Technol.*, 2008, **19**, 647–657.
35 J. P. Gong, Y. Katsuyama, T. Kurokawa and Y. Osada, *Adv. Mater.*, 2003, **15**, 1155–1158.
36 W. B. Wang and A. Q. Wang, *Carbohydr. Polym.*, 2010, **80**, 1028–1036.
37 J. H. Ma, Y. J. Xu, B. Fan and B. R. Liang, *Eur. Polym. J.*, 2007, **43**, 2221–2228.
38 J. Y. Sun, X. Zhao, W. R. K. Illeperuma, O. Chaudhuri, K. H. Oh, D. J. Mooney, J. J. Vlassak and Z. Suo, *Nature*, 2012, **489**, 133–136.
39 X. Y. Gao, Y. Cao, X. F. Song, Z. Zhang, X. L. Zhuang, C. L. He and X. S. Chen, *Macromol. Biosci.*, 2014, **14**, 565–575.
40 Y. Q. Chen, L. B. Chen, H. Bai and L. Li, *J. Mater. Chem. A*, 2013, **1**, 1992–2001.
41 D. L. Han and L. F. Yan, *ACS Sustainable Chem. Eng.*, 2013, **2**, 296–300.
42 W. B. Wang and A. Q. Wang, *Polym. Adv. Technol.*, 2011, **22**, 1602–1611.
43 G. Crini, *Prog. Polym. Sci.*, 2005, **30**, 38–70.
44 M. R. Guilherme, A. V. Reis, S. H. Takahashi, A. F. Rubira, J. P. A. Feitosa and E. C. Muniz, *Carbohydr. Polym.*, 2005, **61**, 464–471.
45 S. Kiatkamjornwong, W. Chomsaksakul and M. Sonsuk, *Radiat. Phys. Chem.*, 2000, **59**, 413–427.
46 L. E. Rioux, S. L. Turgeon and M. Beaulieu, *Carbohydr. Polym.*, 2007, **69**, 530–537.
47 J. H. Kim, S. B. Lee, S. J. Kim and Y. M. Lee, *Polymer*, 2002, **43**, 7549–7558.
48 F. L. Mi, Y. C. Tan, H. F. Liang and H. W. Sung, *Biomaterials*, 2002, **23**, 181–191.
49 S. C. Chen, Y. C. Wu, F. L. Mi, Y. H. Lin, L. C. Yu and H. W. Sung, *J. Controlled Release*, 2004, **96**, 285–300.
50 J. Zhang, Y. W. Cao, J. C. Feng and P. Y. Wu, *J. Phys. Chem. C*, 2012, **116**, 8063–8068.
51 S. Saber-Samandari, S. Saber-Samandari and M. Gazi, *React. Funct. Polym.*, 2013, **73**, 1523–1530.
52 J. C. Fan, Z. X. Shi, M. Lian, H. Li and J. Yin, *J. Mater. Chem. A*, 2013, **1**, 7433–7443.
53 J. H. Liu, G. S. Chen and M. Jiang, *Macromolecules*, 2011, **44**, 7682–7691.
54 J. F. Zhu, Y. J. Zhu, M. G. Ma, L. X. Yang and L. Gao, *J. Phys. Chem. C*, 2007, **111**, 3920–3926.
55 C. Sartori, D. S. Finch and B. Ralph, *Polymer*, 1997, **38**, 43–51.
56 L. Guo, H. Sato, T. Hashimoto and Y. Ozaki, *Macromolecules*, 2010, **43**, 3897–3902.
57 M. M. Coleman, D. J. Skrovanek, J. Hu and P. C. Painter, *Macromolecules*, 1988, **21**, 59–65.
58 J. Shen, B. Yan, T. Li, Y. Long, N. Li and M. Ye, *Composites, Part A*, 2012, **43**, 1476–1481.
59 K. Haraguchi, R. Farnworth, A. Ohbayashi and T. Takehisa, *Macromolecules*, 2003, **36**, 5732–5741.
60 K. Haraguchi, H.-J. Li, K. Matsuda, T. Takehisa and E. Elliott, *Macromolecules*, 2005, **38**, 3482–3490.
61 H. P. Cong, P. Wang and S. H. Yu, *Chem. Mater.*, 2013, **25**, 3357–3362.
62 L. Guo, H. Sato, T. Hashimoto and Y. Ozaki, *Macromolecules*, 2010, **43**, 3897–3902.